



Article

The Catalase KatA Contributes to Microaerophilic H₂O₂ Priming to Acquire an Improved Oxidative Stress Resistance in *Staphylococcus aureus*

Nico Linzner, Vu Van Loi and Haike Antelmann *

Institute of Biology-Microbiology, Freie Universität Berlin, 14195 Berlin, Germany

* Correspondence: haike.antelmann@fu-berlin.de; Tel.: +49-(0)30-838-51221

Abstract: *Staphylococcus aureus* has to cope with oxidative stress during infections. In this study, *S. aureus* was found to be resistant to 100 mM H₂O₂ during aerobic growth. While KatA was essential for this high aerobic H₂O₂ resistance, the peroxiredoxin AhpC contributed to detoxification of 0.4 mM H₂O₂ in the absence of KatA. In addition, the peroxiredoxins AhpC, Tpx and Bcp were found to be required for detoxification of cumene hydroperoxide (CHP). The high H₂O₂ tolerance of aerobic *S. aureus* cells was associated with priming by endogenous H₂O₂ levels, which was supported by an oxidative shift of the bacillithiol redox potential to −291 mV compared to −310 mV in microaerophilic cells. In contrast, *S. aureus* could be primed by sub-lethal doses of 100 μM H₂O₂ during microaerophilic growth to acquire an improved resistance towards the otherwise lethal triggering stimulus of 10 mM H₂O₂. This microaerophilic priming was dependent on increased KatA activity, whereas aerobic cells showed constitutive high KatA activity. Thus, KatA contributes to the high H₂O₂ resistance of aerobic cells and to microaerophilic H₂O₂ priming in order to survive the subsequent lethal triggering doses of H₂O₂, allowing the adaptation of *S. aureus* under infections to different oxygen environments.



Citation: Linzner, N.; Loi, V.V.; Antelmann, H. The Catalase KatA Contributes to Microaerophilic H₂O₂ Priming to Acquire an Improved Oxidative Stress Resistance in *Staphylococcus aureus*. *Antioxidants* **2022**, *11*, 1793. <https://doi.org/10.3390/antiox11091793>

Academic Editor: Elena Forte

Received: 8 August 2022

Accepted: 7 September 2022

Published: 12 September 2022

Publisher's Note: MDPI stays neutral with regard to jurisdictional claims in published maps and institutional affiliations.



Copyright: © 2022 by the authors. Licensee MDPI, Basel, Switzerland. This article is an open access article distributed under the terms and conditions of the Creative Commons Attribution (CC BY) license (<https://creativecommons.org/licenses/by/4.0/>).

Keywords: *Staphylococcus aureus*; H₂O₂ resistance; priming; KatA; AhpC; Tpx; Bcp

1. Introduction

Staphylococcus aureus is a major human pathogen that can cause local skin and soft tissue infections, as well as life-threatening diseases, such as septicaemia, endocarditis, necrotizing pneumonia and osteomyelitis [1–3]. During infections, *S. aureus* has to cope with reactive oxygen species (ROS), such as superoxide anion (O₂^{•−}) and hydrogen peroxide (H₂O₂) [4], which are produced during the oxidative burst of activated macrophages and neutrophils to kill the invading pathogen [5–8]. The NADPH oxidase (NOX2) in the phagosomal membrane catalyses the one-electron transfer to molecular oxygen (O₂) to generate O₂^{•−}, which is dismutated to H₂O₂ either spontaneously or by superoxide dismutases (SODs), including the extracellular SOD3 [6,8–11]. Both SOD3 and NOX2 are contained in secretory vesicles in macrophages and neutrophils and the fusion of these vesicles with phagosomes during phagocytosis might provide a mechanism for catalysed H₂O₂ production [11]. However, in neutrophils, the myeloperoxidase MPO is released from azurophilic granula into the phagosomal lumen, catalysing the dismutation of O₂^{•−} to H₂O₂ upon infection [6]. MPO further converts H₂O₂ with chloride to the highly reactive hypochlorous acid (HOCl), which is the most potent oxidant and microbicidal agent released by activated neutrophils [6,9,10]. In addition, *S. aureus* encounters endogenous ROS during aerobic respiration due to the stepwise one-electron transfer reactions to O₂, leading to production of O₂^{•−} and H₂O₂ [12]. In the Fenton reaction, H₂O₂ reacts with free Fe²⁺ to generate the highly toxic hydroxyl radical (OH[•]), which can damage all cellular macromolecules, resulting in oxidation of proteins, lipids and carbohydrates [12–14]. However, H₂O₂ and HOCl can also function in redox signalling to activate or inactivate specific redox-sensitive

regulators, which control defence mechanisms and confer resistance against the oxidants in bacterial pathogens [14,15].

S. aureus uses various enzymatic and non-enzymatic ROS and HOCl detoxification systems, such as a unique catalase (KatA), several peroxiredoxins (AhpC, Tpx, Bcp) and the low-molecular-weight (LMW) thiol bacillithiol (BSH) [14,16]. BSH associates with the bacilliredoxin/BSH/YpdA redox pathway to regenerate oxidized protein thiols and bacillithiol disulfide (BSSB) [16]. We previously constructed a Brx-roGFP2 fused biosensor to monitor the changes in the BSH redox potential (E_{BSH}) under oxidative stress in *S. aureus* [17]. This study already revealed that *S. aureus* is highly resistant to 100 mM H_2O_2 , since the Brx-roGFP2 biosensor responded only weakly to high H_2O_2 levels, leading to small E_{BSH} changes [17]. The catalase KatA was identified as the major H_2O_2 detoxification enzyme, which conferred the constitutive H_2O_2 -resistant phenotype to aerobically grown *S. aureus* cells [18,19]. KatA is also important for nasal colonization and mediates protection under macrophage and neutrophil infections [18,20–22]. The peroxiredoxin AhpCF showed compensatory roles in resistance to H_2O_2 and organic hydroperoxides (OHPs) and contributed to nasal colonization [20]. OHPs (ROOH) are generated during oxidation of polyunsaturated fatty acids of eukaryotic membrane lipids and are reduced by peroxiredoxins to their corresponding organic alcohols [23].

In general, AhpC, Tpx and Bcp can be classified into typical (AhpC) or atypical (Tpx, Bcp) 2-Cys peroxiredoxins based on their thiol-oxidation mechanism between the peroxidatic (C_P) and resolving Cys (C_R), involving inter- or intramolecular disulfides, respectively [24]. The functions and substrates of AhpC, Tpx and Bcp have been previously studied in *Escherichia coli*. AhpC detoxification of H_2O_2 leads to formation of an oxidized AhpC dimer, which aggregates to an oligomer with chaperone functions [24,25]. Regeneration of AhpC requires the NADPH-dependent flavin disulfide reductase AhpF as a redox partner [24,25]. The thiol-peroxidase Bcp of *E. coli* is induced by H_2O_2 , OHPs and during aerobic growth and confers resistance against H_2O_2 and OHP stress [26]. The thiol-peroxidase Tpx of *E. coli* has been shown to catalyse detoxification of H_2O_2 and OHPs in vitro and is recycled by the Trx/TrxR system [27,28]. In *S. aureus*, Tpx responds strongly to H_2O_2 and other thiol-reactive compounds and was oxidized in the redox proteome under HOCl stress [14,29]. However, the detailed functions of the peroxiredoxins AhpC, Tpx and Bcp in peroxide resistance, detoxification and survival have not been studied thus far in *S. aureus*.

In *S. aureus*, transcription of *katA*, *ahpCF* and *bcp* is strongly induced only by high levels of 10 mM H_2O_2 and controlled by the peroxide-responsive PerR repressor [18,20,30]. In *Bacillus subtilis*, KatA is also a member of the PerR regulon but already inducible by sub-lethal doses of 100 μ M H_2O_2 [31,32]. Pretreatment of *B. subtilis* cells with sub-lethal H_2O_2 as “priming stimulus” confers improved resistance towards subsequent lethal H_2O_2 doses, termed as “triggering stimulus”, which are encountered as future stress [33,34]. These terms and abbreviations—priming (P), priming plus triggering (PT) and triggering (T)—were previously introduced within our project SFB973, which was directed to priming and memory of stress responses in different organisms, including bacteria, fungi and plants [35]. In *B. subtilis*, the H_2O_2 priming effect was shown to be mediated by KatA, which is induced by a mild stress to prepare the cells for better survival when faced with future lethal oxidative stress [33]. Similarly, H_2O_2 priming for improved resistance towards the triggering stimulus was dependent on the OxyR-dependent enzymes KatG and AhpCF in *E. coli* and *Salmonella Typhimurium* [32,36,37]. Although *S. aureus* exhibits constitutive H_2O_2 resistance during aerobic growth, it is unknown whether priming for improved H_2O_2 resistance is possible under aerobic or microaerophilic conditions.

In this study, we used growth and survival phenotype analyses, Brx-roGFP2 biosensor measurements and transcriptional studies to investigate the functions of KatA and the peroxiredoxins AhpC, Tpx and Bcp in peroxide resistance, detoxification and priming during aerobic and microaerophilic growth. Our results showed that *S. aureus* is H_2O_2 primable for improved resistance only under microaerophilic conditions, which are depen-

dent on KatA. In contrast, aerobic growth already leads to increased levels of ROS, which causes KatA-dependent aerobic priming for constitutive H₂O₂ resistance. While KatA confers H₂O₂ resistance in *S. aureus*, the peroxiredoxins AhpC, Tpx and Bcp were shown to contribute to survival and resistance under CHP stress and regeneration of reduced E_{B_{SH}} upon recovery from CHP stress.

2. Materials and Methods

2.1. Bacterial Strains, Growth and Survival Assays

Bacterial strains, plasmids and primers are described in Tables S1–S3. For genetic manipulation, *E. coli* was cultivated in Luria Broth (LB) medium. *S. aureus* COL strains were grown in RPMI medium to an optical density at 500 nm (OD₅₀₀) of 0.5 and exposed to H₂O₂, cumene hydroperoxide (CHP) or hypochlorous acid (HOCl), followed by determination of colony-forming units (CFUs) in survival assays as previously described [38]. Each experiment was performed in at least three independent biological replicates and the results are presented as mean values with standard deviations (SD) from all biological replicates, as indicated in each figure legend. Statistical analysis was performed using Student's unpaired two-tailed *t*-test with the software Graph Prism. The biochemical compounds were purchased from Sigma Aldrich. The HOCl concentration was determined as previously described [39].

2.2. Construction of the *S. aureus* COL $\Delta katA$, $\Delta ahpC$, $\Delta ahpC\Delta katA$, Δtpx , Δbcp and $\Delta perR$ Mutants and Complemented Strains

The *S. aureus* COL $\Delta katA$ mutant and *katA* complemented strains were previously constructed [40]. The *S. aureus* $\Delta ahpC$, Δtpx , Δbcp and $\Delta perR$ deletion mutants were constructed using the temperature-sensitive *E. coli*-*S. aureus* shuttle vector pMAD as previously described [41]. In brief, 500 bp of the up- and downstream flanking regions of the specific genes were fused by PCR, digested with *Bgl*II and *Sal*I and ligated into pMAD. The constructs were electroporated into the restriction-negative *S. aureus* RN4220, followed by phage transduction using phage 81 into *S. aureus* COL [42]. For construction of the $\Delta ahpC\Delta katA$ double mutant, the plasmid pMAD- $\Delta katA$ of *S. aureus* RN4220-pMAD- $\Delta katA$ was transduced by the phage 81 into the *S. aureus* COL $\Delta ahpC$ mutant. Selection of the $\Delta ahpC$, Δbcp , Δtpx , $\Delta perR$ and $\Delta ahpC\Delta katA$ deletion mutants was performed as previously described [38].

Construction of the His-tagged *S. aureus* *ahpC*, *bcp* and *tpx* complemented strains was performed using the plasmid pRB473 as previously described [17]. The genes were cloned into pRB473 after digestion with *Bam*HI and *Kpn*I/*Sac*I, resulting in plasmids pRB473-*ahpC*-His, pRB473-*bcp*-His and pRB473-*tpx*-His, which were transduced in the $\Delta ahpC$, Δbcp and Δtpx deletion mutants. In addition, the plasmid pRB473-*brx-roGFP2* [17] was introduced into the *S. aureus* COL $\Delta katA$, $\Delta ahpC$, $\Delta ahpC\Delta katA$, Δtpx and Δbcp deletion mutants to construct the Brx-roGFP2 biosensor expressing catalase- and peroxiredoxin-deficient mutant strains.

2.3. Priming and Triggering Experiments

For priming and triggering, the *S. aureus* strains were grown aerobically under vigorous agitation in shake flasks in a shaking water bath at 150 rpm or microaerophilically in 50 mL Falcon tubes including 40 mL cultures with closed lids without shaking, as in previous publications [43,44]. At an OD₅₀₀ of 0.3, naïve *S. aureus* cells were primed by adding sub-lethal doses of 0.1 or 1 mM H₂O₂, respectively, to the bacterial culture for ~30 min. Subsequently, the lethal triggering doses of 10 or 40 mM H₂O₂, respectively, were added to the primed bacterial cultures, followed by counting of CFUs after 2 and 4 h of growth. For triggering only, naïve cells were treated with 10 or 40 mM H₂O₂ at an OD₅₀₀ of 0.4, followed by counting of CFUs after 2 and 4 h of growth.

2.4. Brx-roGFP2 Biosensor Measurements

To monitor the E_{BSH} changes after H_2O_2 and CHP stress, we used the Brx-roGFP2 biosensor expressing WT, $\Delta katA$, $\Delta ahpC$, $\Delta ahpC\Delta katA$, Δtpx and Δbcp mutant strains and performed injection assays with the oxidants. For measurements of Brx-roGFP2 oxidation during microaerophilic and aerobic H_2O_2 priming and triggering experiments, the *S. aureus* COL strain expressing Brx-roGFP2 was cultivated in LB medium to an OD_{540} of 0.3 and challenged with the priming dose of 0.1 mM H_2O_2 for 30 min, followed by the triggering dose of 10 mM H_2O_2 , as described above. Samples were harvested from *S. aureus* cells in the naïve (C), primed (P), primed and triggered (PT) and triggered-only (T) states, alkylated with 10 mM N-ethylmaleimide (NEM), washed and resuspended in PBS with 10 mM NEM. The Brx-roGFP2 oxidation degree (OxD) and E_{BSH} changes were determined in the *S. aureus* strains during oxidant injection or in samples harvested at C, P, PT and T as previously described [17,45]. For fully reduced and oxidized controls, biosensor strains were treated with 10 mM DTT and 5 mM diamide, respectively. The Brx-roGFP2 fluorescence emission was measured at 510 nm after excitation at 405 and 488 nm using the CLARIOstar microplate reader (BMG Labtech). The OxD of the Brx-roGFP2 biosensor was determined for each sample and normalized to fully reduced and oxidized controls as previously described [17,45].

2.5. Northern Blot Analyses

To analyze transcription of *katA*, *dps* and *ahpCF* in the *S. aureus* COL WT, $\Delta katA$, $\Delta ahpC$ and $\Delta perR$ mutants using Northern blots, the *S. aureus* strains were grown in RPMI medium and harvested during the log phase at an OD_{500} of 0.4. To investigate *katA* and *ahpC* induction in the priming and triggering experiments, *S. aureus* WT cells were harvested in the naïve (C), primed (P), primed and triggered (PT) and triggered-only (T) states, as explained in the figure legends. RNA isolation was performed using the acid phenol extraction protocol as described previously [46]. Northern blot hybridizations were conducted using digoxigenin-labelled antisense RNA probes for *katA*, *ahpC* and *dps* that were synthesized in vitro using T7 RNA polymerase and the corresponding primers *katA*-NB-for/rev and *ahpC*-NB-for/rev, as previously described [46]. The *dps* antisense RNA probe was constructed previously [44].

2.6. Determination of the Catalase Activity Using Native PAGE and Diaminobenzidine Staining

To analyze catalase activities in *S. aureus* COL strains, protein extracts were prepared under native conditions and 50 μg of each sample was separated by non-denaturing 10% polyacrylamide gel electrophoresis. The gel was stained for catalase activity using 50 $\mu\text{g}/\text{mL}$ horseradish peroxidase coupled with 5 mM H_2O_2 and 0.5 mg/mL diaminobenzidine, as described previously [47,48].

3. Results

3.1. *S. aureus* Exhibits KatA-Dependent H_2O_2 Resistance during Aerobic Growth

To investigate the roles of the catalases and peroxiredoxins in the constitutive H_2O_2 resistance of *S. aureus* COL, phenotype analyses of the $\Delta katA$, $\Delta ahpC$, $\Delta ahpC\Delta katA$, Δtpx and Δbcp mutants and the complemented strains were performed during the aerobic growth under H_2O_2 stress (Figure 1; Figures S1 and S2). In agreement with previous findings [20], the $\Delta katA$ mutant was strongly impaired in growth after exposure to 10 mM H_2O_2 and did not survive doses of 40 mM H_2O_2 (Figure 1A,E). The *S. aureus* COL wild type (WT) was able to grow with low doses of 1 mM H_2O_2 and survived to 330 and 725% after 2 and 4 h, respectively (Figure 1F; Figure S1B). However, the $\Delta katA$ mutant was hypersensitive to peroxide stress, since the growth was inhibited by 0.4 and 1 mM H_2O_2 and only 32% and 4% of cells survived the 1 mM H_2O_2 treatment after 2 and 4 h, respectively (Figure 1F; Figure S1B). Complementation of the $\Delta katA$ mutant with pRB473-encoded *katA* could only partially restore the H_2O_2 resistance to WT level after treatment with 0.4–1 mM H_2O_2 (Figure 1F; Figure S1A–C). This incomplete recovery of the WT resistance was due to lower

catalase activity in the *katA* complemented strain, as confirmed using the diaminobenzidine gel staining method (Figure S1D).

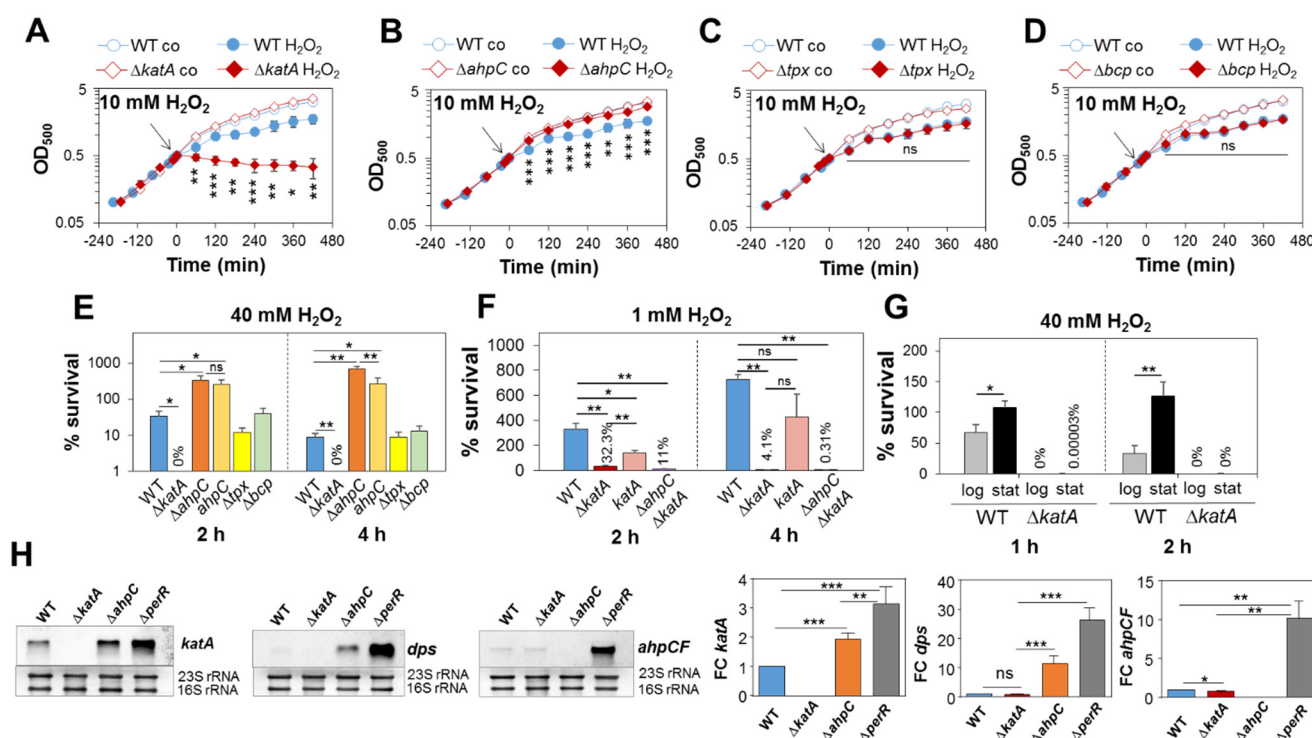


Figure 1. KatA confers strong H₂O₂ resistance during aerobic growth, while Tpx and Bcp are not required for H₂O₂ resistance. (A–D) Growth curves of *S. aureus* COL WT, $\Delta katA$ (A), $\Delta ahpC$ (B), Δtpx (C) and Δbcp mutants (D) in RPMI medium before (co) and after exposure to 10 mM H₂O₂ at an OD₅₀₀ of 0.5. (E) Survival rates were determined as CFU counts for *S. aureus* COL WT, $\Delta katA$, $\Delta ahpC$, Δtpx and Δbcp mutants and the *ahpC* complemented strain at 2 and 4 h after treatment with 40 mM H₂O₂. (F) Survival rates were analysed for the WT, $\Delta katA$ and $\Delta ahpC \Delta katA$ mutants and the *katA* complemented strain (*katA*) after 2 and 4 h of exposure to 1 mM H₂O₂ based on CFU counts. (G) *S. aureus* COL WT and $\Delta katA$ mutant cells were exposed to 40 mM H₂O₂ during the log and stationary phases at OD₅₀₀ of 0.5 and 2–3, respectively. In (E–G), the survival rates were calculated relative to the untreated control, which was set to 100%. Mean values and standard deviation (SD) from three to four biological replicates are shown. (H) Northern blot analyses of the *katA*, *dps* and *ahpCF* specific transcripts in the *S. aureus* WT, $\Delta katA$, $\Delta ahpC$ and $\Delta perR$ mutants. The methylene blue stains below the Northern blot images denote the bands of the 16S and 23S rRNAs used as RNA loading controls. Quantification of the intensities of the Northern blot bands was performed from two biological and three technical replicates using Image J and is shown in the diagrams as fold changes (FCs) of induction of the *katA*, *dps* and *ahpCF* transcripts in the mutants relative to the WT. Error bars represent the SD. The statistics were analysed using Student’s unpaired two-tailed *t*-test in Graph Prism. Symbols: ns $p > 0.05$, * $p \leq 0.05$, ** $p \leq 0.01$ and *** $p \leq 0.001$.

In addition, the H₂O₂ resistance of WT cells was 1.5–4-fold further enhanced during the stationary phase, whereas the $\Delta katA$ mutant did not survive 40 mM H₂O₂ during the log and stationary phases (Figure 1G). These data indicate that KatA also contributes to the stationary-phase H₂O₂ resistance in *S. aureus*. In contrast, the peroxiredoxin-deficient *S. aureus* Δtpx and Δbcp mutants were not impaired in growth or survival after exposure to 10 and 40 mM H₂O₂ (Figure 1C–E). However, the $\Delta ahpC$ mutant displayed an increased H₂O₂ resistance (Figure 1B,E), which was mediated by the PerR-dependent up-regulation of KatA in the $\Delta ahpC$ mutant, as shown previously [20]. To validate the derepression of PerR regulon genes in the $\Delta ahpC$ mutant, we analysed the transcription of *katA* and the miniferritin-encoding *dps* gene, since both were strongly up-regulated under different

thiol-stress conditions in the transcriptome of *S. aureus* WT cells [43,49,50]. The Northern blot results revealed the twofold up-regulation of *katA*, while *dps* transcription was induced at an 11-fold higher rate in the Δ *ahpC* mutant, supporting the derepression of both PerR regulon genes in the Δ *ahpC* mutant under non-stress conditions (Figure 1H).

However, the H₂O₂-resistant phenotype of the Δ *ahpC* mutant could not be reversed to WT levels in growth and survival assays upon exposure to 10 and 40 mM H₂O₂ in the *ahpC* complemented strain (Figures 1E and S2A). This lack of complementation might be caused by the lower plasmid-borne AhpC expression compared to the highly abundant AhpC in WT cells, as previously observed in the proteome [51]. The catalase activity was higher in the Δ *ahpC* mutant and *ahpC* complemented strain than in the WT, explaining the high H₂O₂ resistance upon complementation (Figure S2B). To confirm whether KatA and AhpC play additive roles in H₂O₂ resistance, the growth and survival of the Δ *ahpC* Δ *katA* double mutant was analysed. In agreement with previous data, the Δ *ahpC* Δ *katA* mutant showed a slower aerobic growth (Figure S3A) [20] and displayed 3-fold and 13-fold reduced survival rates after exposure to 1 mM H₂O₂ for 2 h and 4 h, respectively, as compared to the Δ *katA* mutant (Figure 1F).

Taken together, these results indicate that KatA plays the major role of conferring strong H₂O₂ resistance to aerobic *S. aureus* cells during the log and the stationary phases, whereas AhpC makes a minor contribution to the H₂O₂ resistance during the aerobic growth. Thus, KatA was identified as major determinant of the H₂O₂ resistance in growing and non-growing *S. aureus* cells.

3.2. The Δ *katA* Mutant Shows a Strong Oxidative Shift in the E_{BSH} after H₂O₂ Stress and Is Impaired in Its Regeneration of the Reduced State, as Revealed by the Brx-roGFP2 Biosensor

To monitor the changes in the E_{BSH} in the catalase- and peroxiredoxin-deficient mutants, we measured the Brx-roGFP2 biosensor responses after H₂O₂ stress in the WT and mutant strains. Due to the strong aerobic H₂O₂ resistance of *S. aureus* WT cells, the Brx-roGFP2 biosensor responded only weakly to 10 mM H₂O₂ in our previous studies [17]. Thus, we first used 100 mM H₂O₂ for WT cells, leading to fast biosensor oxidation and regeneration of the reduced state of E_{BSH} within two hours, as in our previous studies (Figure 2A) [17].

No increased biosensor oxidation was measured in WT cells after exposure to 1 mM H₂O₂ (Figure 2B). In contrast to WT cells, the biosensor was fully and constitutively oxidized by 1 and 100 mM H₂O₂ in the Δ *katA* mutant, indicated by an impaired regeneration of reduced E_{BSH} (Figure 2A,B). The *katA* mutant was only able to recover the reduced state of E_{BSH} after treatment with 0.4 mM H₂O₂ (Figure 2C), suggesting that this low H₂O₂ level might be detoxified by AhpC. In support of this hypothesis, the Brx-roGFP2 biosensor was quickly oxidized and strongly delayed in the recovery of reduced E_{BSH} after exposure to 0.4 mM H₂O₂ in the Δ *ahpC* Δ *katA* double mutant (Figure S3B). In contrast, the Δ *ahpC*, Δ *tpx* and Δ *bcp* mutants showed similar H₂O₂ responses and regeneration of reduced E_{BSH} compared to the WT (Figure 2D–F). The biosensor results confirmed the hypersensitivities of the Δ *katA* and Δ *ahpC* Δ *katA* mutants towards H₂O₂ stress, supporting that KatA was responsible for the rapid detoxification of 100 mM of H₂O₂ and regeneration of E_{BSH} in *S. aureus* WT cells, while AhpC could only detoxify low levels of 0.4 mM H₂O₂ in the absence of KatA. However, the peroxiredoxins Tpx and Bcp were not essential for H₂O₂ detoxification in *S. aureus* WT cells.

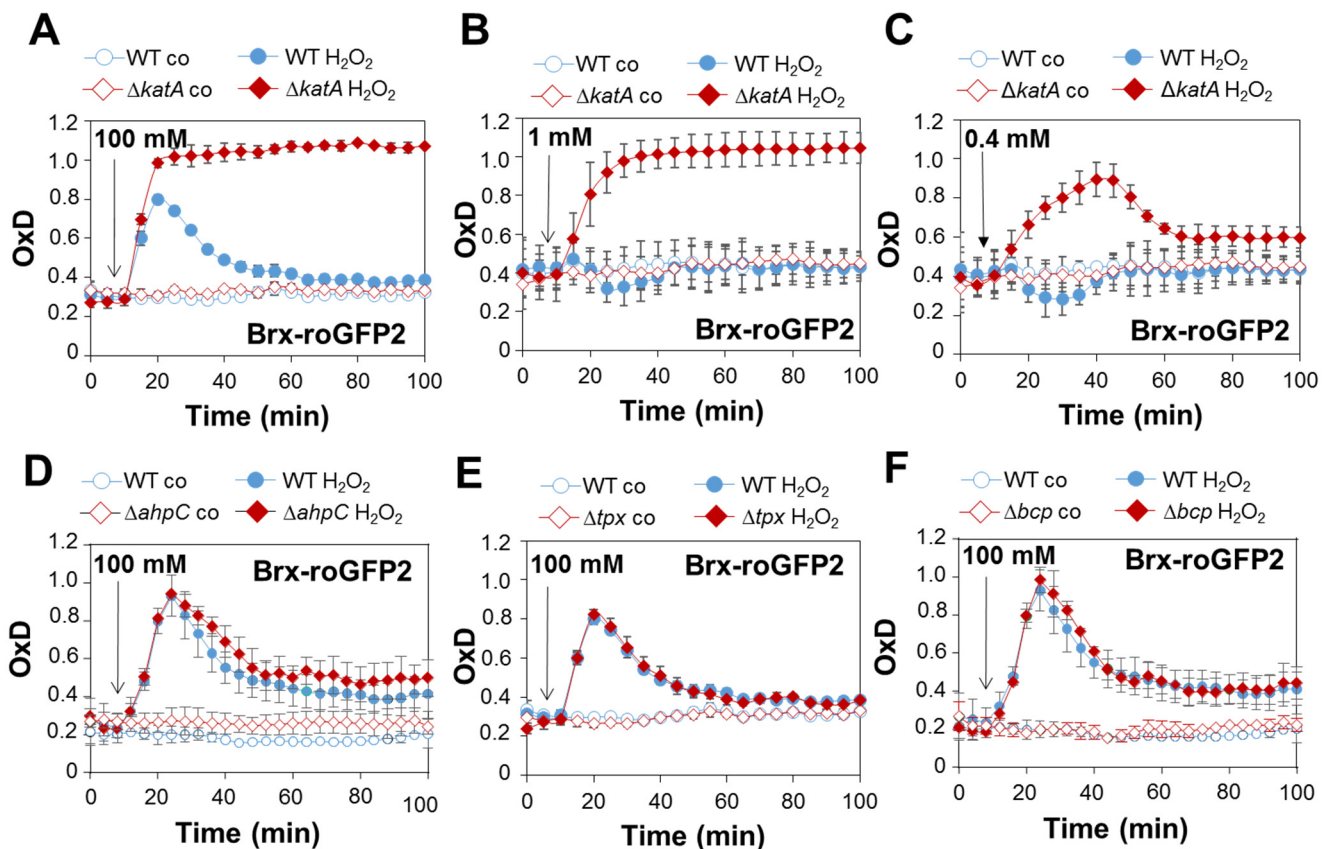


Figure 2. The $\Delta katA$ mutant can only detoxify 0.4 mM H₂O₂ stress, as revealed by the Brx-roGFP2 biosensor in *S. aureus*. (A–F) Brx-roGFP2 biosensor responses to 100, 1 and 0.4 mM H₂O₂ were monitored in the *S. aureus* COL WT, $\Delta katA$ (A–C), $\Delta ahpC$ (D), Δtpx (E) and Δbcp mutants (F) expressing Brx-roGFP2 from plasmid pRB473. H₂O₂ injection assays were performed in microplates using the CLARIOstar microplate reader, as described previously [45]. The oxidation degrees (OxD) of the Brx-roGFP2 responses were calculated based on the 405/488 nm excitation ratios and normalized to fully reduced (DTT-treated) and fully oxidized (diamide-treated) controls, as described previously [45]. Mean values and SD of the OxD values are presented from three independent biological replicates.

3.3. *S. aureus* Shows KatA-Dependent Microaerophilic H₂O₂ Priming to Acquire an Improved Resistance towards Lethal H₂O₂ Doses

The previous data revealed that KatA confers strong H₂O₂ resistance during aerobic growth. However, the role of KatA in the priming of *S. aureus* for improved H₂O₂ resistance during microaerophilic conditions was not investigated. Thus, the *S. aureus* WT and the $\Delta katA$ mutant were grown under microaerophilic conditions to the log phase and primed with 0.1 mM H₂O₂ for 30 min, followed by triggering with 10 mM H₂O₂ (Figure 3A). The growth and survival were analysed in naïve (C), primed (P), primed and triggered (PT) and triggered bacteria (T) (Figure 3A).

The primed *S. aureus* WT and $\Delta katA$ mutant (P) were not impaired in growth and survival under 0.1 mM H₂O₂ (Figure 3B–E). However, the primed and triggered WT (PT) could acquire an improved resistance towards the triggering stimulus of 10 mM H₂O₂ compared to the triggering-only state (T) (Figure 3B,D). Specifically, PT bacteria showed survival rates of 52–72%, whereas T bacteria were almost killed and survived only to <0.07% after 10 mM H₂O₂ treatment. This indicates that *S. aureus* is primable for improved oxidative stress resistance during microaerophilic growth (Figure 3B,D). However, in contrast to the WT, the primed $\Delta katA$ mutant strain was unable to acquire the improved resistance towards otherwise lethal doses of 10 mM H₂O₂ under microaerophilic conditions (Figure 3C,E). Both PT and T bacteria of the $\Delta katA$ mutant were strongly impaired in

growth and completely killed after treatment with 10 mM H₂O₂ as a triggering stimulus (Figure 3C,E).

However, due to its lower catalase activity from plasmid-based KatA expression (Figure S1D), the *katA* complemented strain did not recover the improved H₂O₂ resistance upon microaerophilic priming, resulting in growth inhibition and killing of PT and T bacteria (Figure S4). Overall, these results indicate that KatA is responsible for *S. aureus* priming for improved resistance against upcoming lethal H₂O₂ stress under microaerophilic conditions. Thus, KatA confers the constitutive resistance during aerobic growth and prepares *S. aureus* for future oxidative stress under microaerophilic conditions.

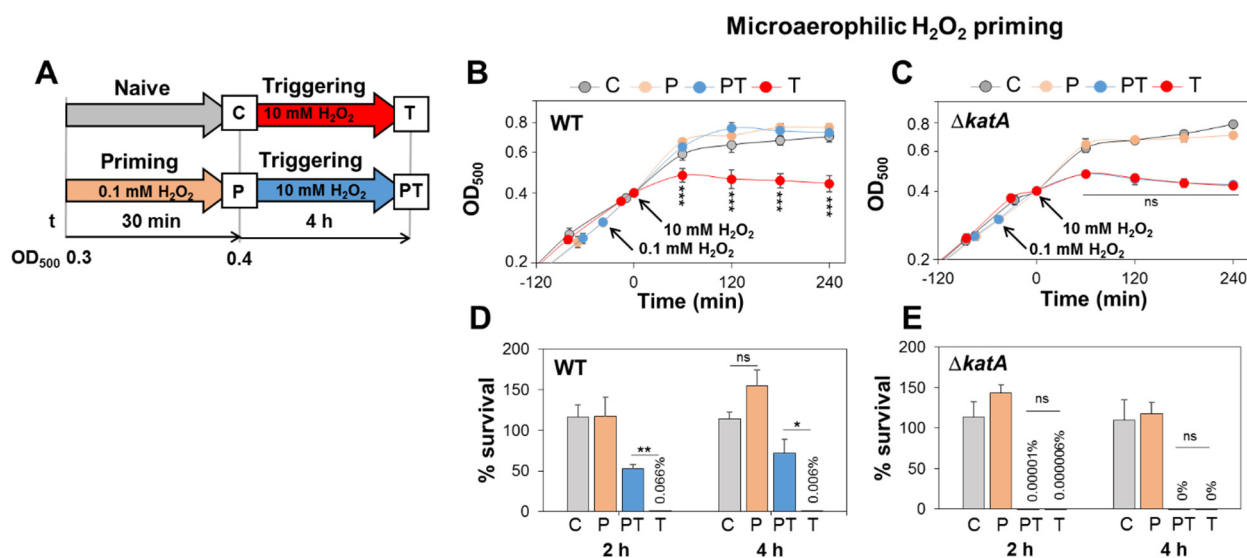


Figure 3. Microaerophilic H₂O₂ priming confers improved resistance against otherwise lethal H₂O₂, which depends on KatA. (A) Setup for microaerophilic priming and triggering experiments. The *S. aureus* WT and *ΔkatA* mutant strains were grown microaerophilically and primed during the log phase with 0.1 mM H₂O₂ for ~30 min (P), followed by treatment with 10 mM H₂O₂ as a triggering stimulus (PT). The growth curves (B,C) and survival rates (D,E) were measured in naïve (C), primed (P), primed and triggered (PT) and triggered-only bacteria (T). The survival rates were calculated after 2 and 4 h of H₂O₂ stress relative to untreated control cells. The results are from three to four biological replicates. Error bars represent the SD. The statistics were calculated using Student's unpaired two-tailed *t*-test in Graph Prism. Symbols: ns *p* > 0.05, * *p* < 0.05, ** *p* ≤ 0.01 and *** *p* ≤ 0.001.

3.4. *S. aureus* Is Not Primable for Improved H₂O₂ Resistance during Aerobic Growth

Next, priming and triggering experiments were performed in aerobically grown *S. aureus* cells to analyse whether the constitutive H₂O₂ resistance could be further enhanced in primed cells (Figure 4). First, we used the same H₂O₂ doses for the priming (0.1 mM) and triggering (10 mM) experiments as applied in the microaerophilic experiments (Figure 4A). As expected, there were no differences in growth and survival between PT and T bacteria after exposure to 10 mM H₂O₂ during the aerobic growth (Figure 4B,C). Both PT and T bacteria were similarly resistant and fully survived the 10 mM H₂O₂ triggering dose. Thus, the constitutive resistance of aerobic *S. aureus* cells towards 10 mM H₂O₂ could not be further enhanced by pre-exposure to the priming stimulus of 0.1 mM H₂O₂ (Figure 4B,C). As shown before, this constitutive H₂O₂ resistance of aerobically grown *S. aureus* cells was dependent on KatA (Figure 1A,E,F).

We further increased the H₂O₂ doses for priming (1 mM H₂O₂) and triggering (40 mM) of *S. aureus* during the aerobic growth (Figure 4D). However, higher priming doses also could not improve the growth and survival of PT bacteria in response to the subsequent 40 mM H₂O₂ stress compared to the T bacteria treated with 40 mM H₂O₂ only (Figure 4E,F).

Both PT and T bacteria were strongly impaired in growth under 40 mM H₂O₂ stress and showed survival rates of <10% after 2 h.

Small survival differences of 4% were observed after 4 h in T versus PT bacteria but not at the 2 h time point (Figure 4F). In conclusion, these different priming setups support that *S. aureus* is not primable for enhanced H₂O₂ resistance under aerobic conditions. We hypothesize that ROS production during aerobic respiration acts as a priming stimulus to induce KatA, which confers the high H₂O₂ resistance.

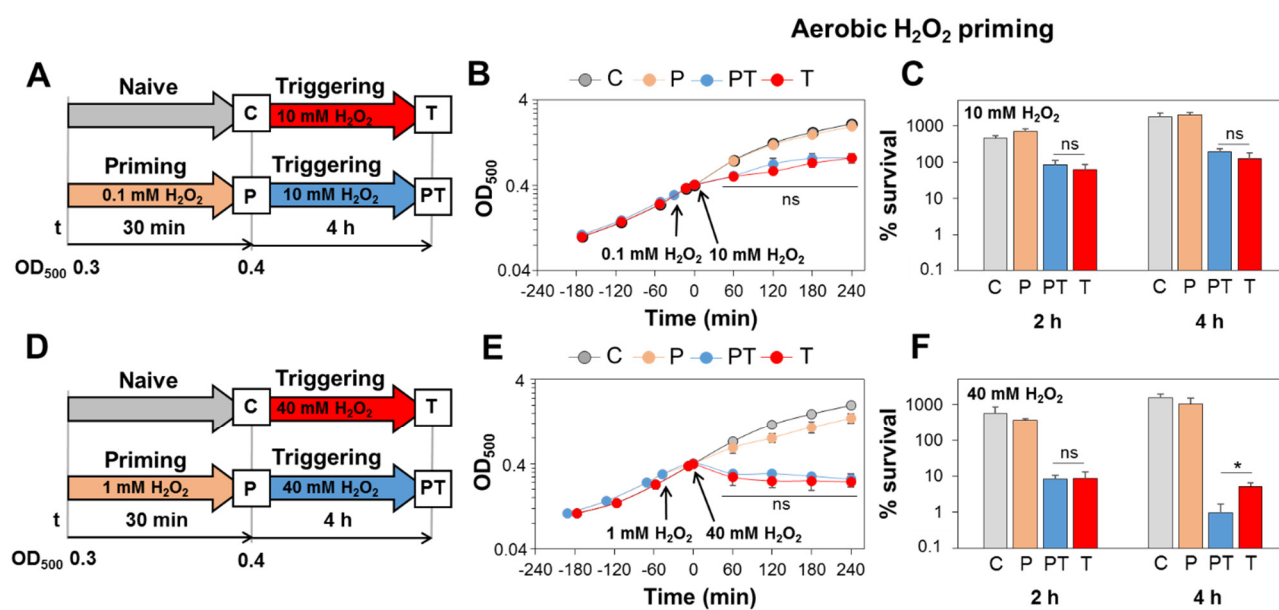


Figure 4. *S. aureus* is not primable for improved H₂O₂ resistance during aerobic growth. (A,D) Setup for aerobic priming and triggering experiments. The aerobically grown *S. aureus* WT was primed during the log phase with either 0.1 mM H₂O₂ (A) or 1 mM H₂O₂ (D) for ~30 min (P) and subsequently treated with either 10 mM H₂O₂ (A) or 40 mM H₂O₂ (D), respectively, as triggering stimuli (PT). The growth curves (B,E) and survival rates (C,F) were measured for naïve (C), primed (P), primed and triggered (PT) and triggered-only bacteria (T). Survival rates of the H₂O₂-treated cells were calculated relative to the untreated control. The results are from three to four biological replicates. Error bars represent the SD. The statistics were calculated using Student's unpaired two-tailed *t*-test in Graph Prism. Symbols: ^{ns} *p* > 0.05 and * *p* < 0.05.

3.5. Microaerophilic H₂O₂ Priming Causes Increased Transcription of *KatA* and Elevated *KatA* Activity, which Confers Improved Resistance towards Lethal H₂O₂ Doses in *S. aureus*

Northern blot analyses were used to study whether microaerophilic H₂O₂ priming induces transcription of the PerR-dependent *katA* gene and the *ahpCF* operon in *S. aureus* (Figure 5). The results revealed that transcription of *katA* was significantly up-regulated by 1.8-fold upon microaerophilic priming with 0.1 mM H₂O₂ (Figure 5B,D), whereas the basal level of *katA* transcription was already higher under aerobic conditions and could not be further induced during aerobic H₂O₂ priming (Figure 5C,E). Transcription of the *ahpCF* operon was not significantly induced during microaerophilic priming (Figure 5B,G). However, transcription of *katA* and *ahpCF* was strongly reduced after triggering by 10 mM H₂O₂ under microaerophilic conditions, since the triggering dose was lethal (Figure 5B,D,G). Transcription of *katA* decreased even in the PT bacteria compared to P cells, which highlights the high efficiency of the KatA protein for fast removal of H₂O₂ in PT bacteria (Figure 5B,D). Under aerobic conditions, PT and T bacteria did not show significantly enhanced transcription of *katA* and *ahpCF*, supporting that the constitutive H₂O₂ resistance could not be further enhanced by pre-exposure to the priming dose (Figure 5C,E,H).

The *katA* transcript levels could be confirmed by catalase activities during the microaerophilic and aerobic priming experiments (Figure 5F). Specifically, the basal activity

of KatA was very low during the microaerophilic growth, whereas aerobic cells showed a constitutive high catalase activity. The KatA activity could be only enhanced upon microaerophilic priming but not during aerobic priming due to the high constitutive resistance (Figure 5F). Further consistent with the Northern blots, the KatA activity decreased strongly in PT and T bacteria during microaerophilic priming. Together, these results reveal that microaerophilic priming induces *katA* transcription and KatA activity, which confers improved resistance against otherwise lethal H₂O₂ stress.

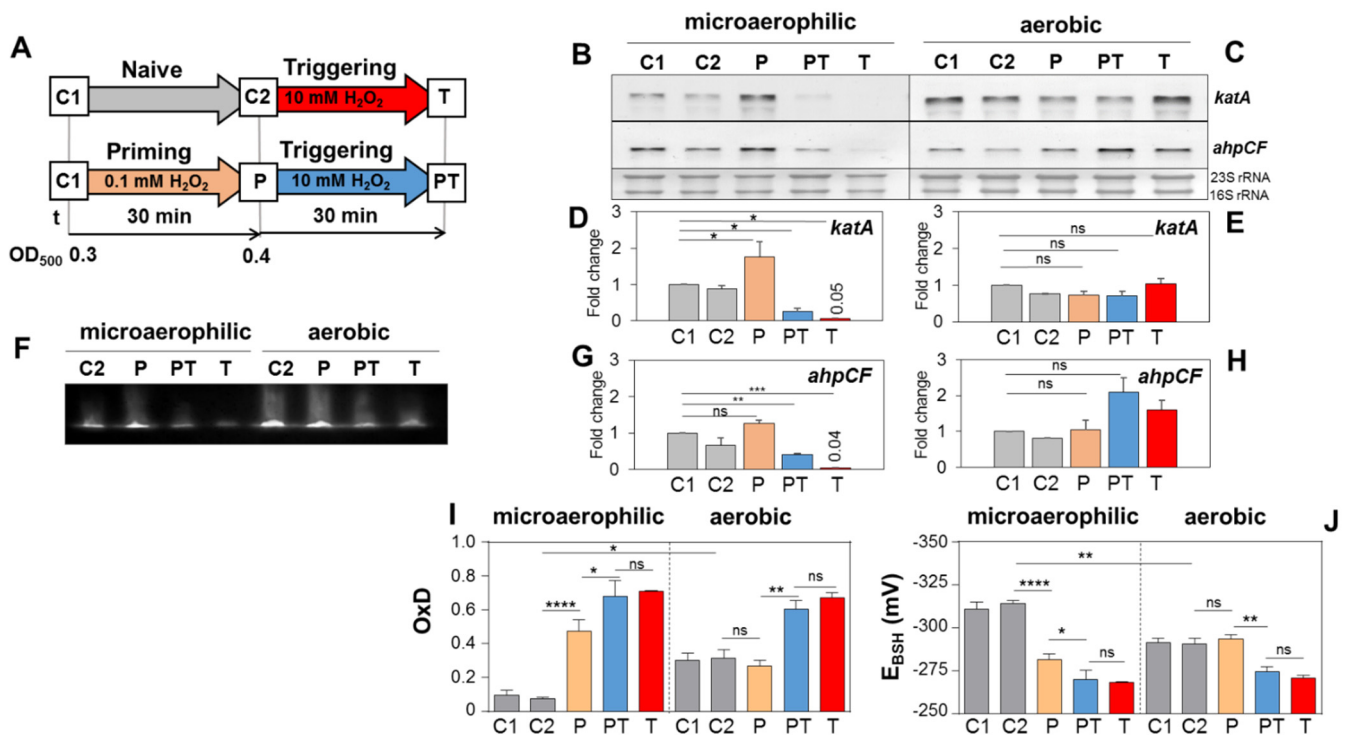


Figure 5. Microaerophilic H₂O₂ priming leads to increased *katA* transcription and KatA activity, as well as fast Brx-roGFP2 biosensor oxidation. (A) The setup for microaerophilic and aerobic priming and triggering experiments included priming with 0.1 mM H₂O₂ and triggering with 10 mM H₂O₂. (B,C) To analyze transcription of *katA* and *ahpCF* using Northern blots, RNA was isolated from *S. aureus* WT cells in the naïve (C1, C2), primed (P), primed and triggered (PT) and triggered (T) states. The band intensities of the *katA* (D,E) and *ahpCF* specific transcripts (G,H) were quantified from two biological replicates using ImageJ. The transcriptional induction of *katA* and *ahpCF* was calculated as fold change relative to the control C1, which was set to 1. Error bars represent the SD. The statistics were calculated using ordinary one-way ANOVA and Dunnett's multiple comparisons test in Graph Prism. Symbols: ^{ns} $p > 0.05$; * $p \leq 0.05$; ** $p \leq 0.01$ and *** $p \leq 0.001$. (F) The catalase activity was analysed in cell extracts of the *S. aureus* WT during microaerophilic and aerobic H₂O₂ priming for C2, P, PT and T states using native PAGE and diaminobenzidine staining. The catalase activity assays were performed in two biological and two technical replicates. (I,J) The response of the Brx-roGFP2 biosensor was measured in *S. aureus* COL grown in LB medium under microaerophilic and aerobic conditions in naïve (C1, C2), primed (P), primed and triggered (PT) and triggered (T) cells. The C1 and C2 samples were harvested at OD₅₀₀ of 0.3 and 0.4, respectively, and the P, PT and T bacteria were harvested after 10 min of H₂O₂ exposure (maximum biosensor oxidation). Samples were blocked with 10 mM NEM and the fluorescence excitation maxima were measured at 405 and 488 nm using the microplate reader. OxD values and the E_{BSH} of Brx-roGFP2 were calculated using the 405/408 nm excitation ratio, as described in the Section 2. Mean values of three biological replicates are shown, error bars represent the SD and p -values were calculated using Student's unpaired two-tailed t -test in Graph Prism software. Symbols: ^{ns} $p > 0.05$; * $p \leq 0.05$; ** $p \leq 0.01$; *** $p \leq 0.001$ and **** $p \leq 0.0001$.

3.6. Microaerophilic H₂O₂ Priming Leads to a Strong Oxidative Shift in the E_{B_{SH}}

We were interested in the E_{B_{SH}} differences between aerobic and microaerophilic growth conditions, supporting the enhanced ROS levels in aerobic cells as endogenous priming stimuli. Moreover, we aimed to analyse the Brx-roGFP2 biosensor response upon microaerophilic priming and triggering to investigate if the KatA induction upon microaerophilic priming is accompanied by a change in the Brx-roGFP2 biosensor oxidation. The comparison of the basal biosensor oxidation revealed a more reducing basal OxD of 0.1 and an E_{B_{SH}} of −310 mV during microaerophilic growth (C1) compared to the OxD of 0.3 and the E_{B_{SH}} of −291 mV during aerobic growth (C1) (Figure 5I,J). Thus, the higher basal oxidation in aerobic cells accounted for the increased ROS level due to aerobic respiration. Upon microaerophilic priming, the Brx-roGFP2 biosensor showed a fivefold increased OxD and an oxidized E_{B_{SH}} of −281 mV, which was further oxidized in PT and T bacteria. In contrast, the biosensor did not respond to aerobic priming and showed increased oxidation only in aerobic PT and T bacteria (Figure 5I,J). These results support that microaerophilic priming leads to an oxidative shift in the E_{B_{SH}} from −310 mV to −281 mV, resulting in increased catalase expression that primes the cells for improved H₂O₂ resistance. Due to the higher basal oxidation in aerobic cells, priming did not change the high E_{B_{SH}} of −291 mV, which is consistent with the constitutive KatA expression (Figure 5I,J). These results on the E_{B_{SH}} differences of ~20 mV between microaerophilic and aerobic cells strongly support that respiratory H₂O₂ primes aerobic cells for constitutive H₂O₂ resistance.

3.7. The Peroxiredoxins AhpC, Tpx and Bcp Mediate CHP Resistance in *S. aureus*

While the role of KatA in aerobic H₂O₂ resistance and microaerophilic H₂O₂ priming was clearly revealed, the peroxiredoxins AhpC, Tpx and Bcp could also function in the resistance to organic hydroperoxides in *S. aureus*. Using growth and survival assays, the phenotypes of the catalase and peroxiredoxin-deficient mutants were analysed after CHP treatment (Figure 6). While the growth of the $\Delta katA$ and Δbcp mutants was not affected by 0.15 mM CHP stress, the CHP-treated $\Delta ahpC$ and Δtpx mutants showed slightly reduced growth rates (Figure 6A–D), which could be restored to WT levels upon complementation (Figure 6E,F). In addition, the $\Delta ahpC$, Δtpx and Δbcp mutants showed significantly decreased survival rates after 4 h of CHP stress, supporting that the peroxiredoxins confer protection against CHP stress in *S. aureus* (Figure 6G). These CHP-sensitive survival phenotypes of the peroxiredoxin-deficient mutants could be restored to WT levels in the *ahpC*, *tpx* and *bcp* complemented strains (Figure 6H). However, the slightly increased CHP resistance of the $\Delta katA$ mutant could not be reverted to WT levels in the *katA* complemented strain (Figure 6G), probably due to the partial complementation by plasmid-based KatA expression (Figure S1D).

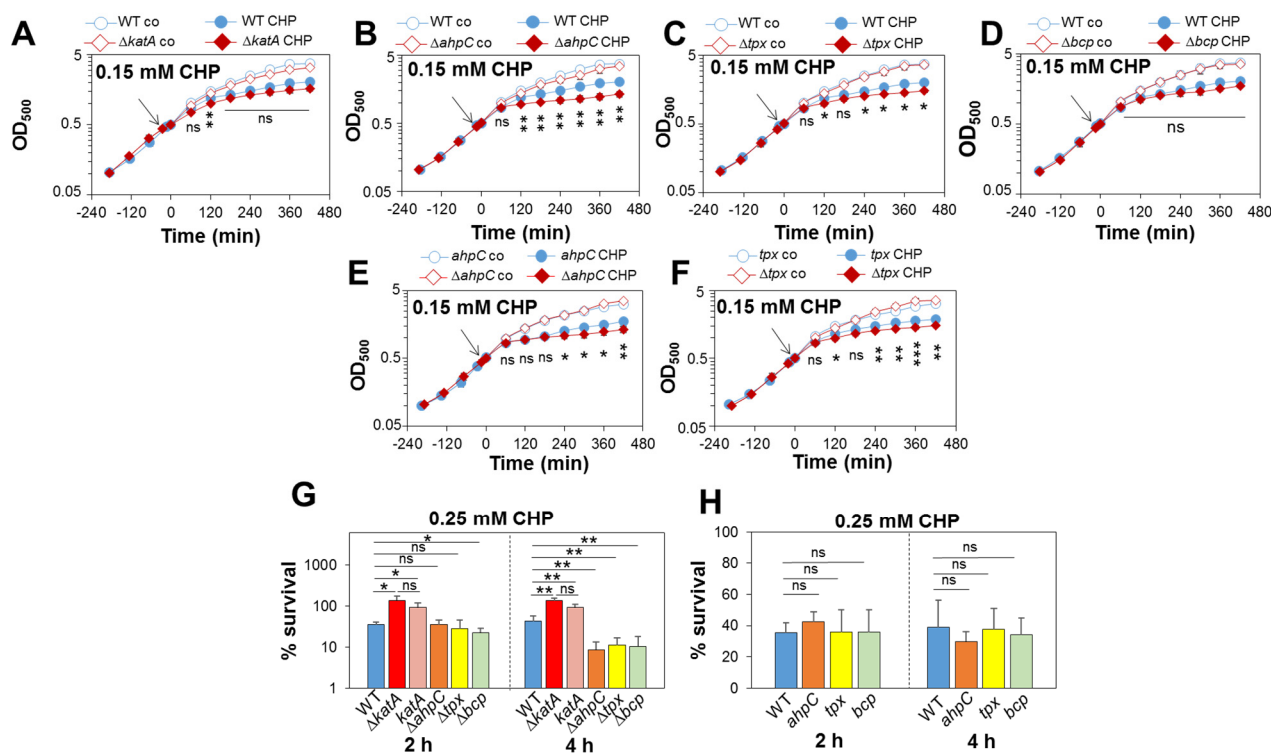


Figure 6. The peroxiredoxins AhpC, Tpx and Bcp contribute to CHP resistance in *S. aureus*. (A–F) Growth phenotypes were analysed for the *S. aureus* COL WT, $\Delta katA$ (A), $\Delta ahpC$ (B), Δtpx (C) and Δbcp mutants (D) and the *ahpC* (E) and *tpx* (F) complemented strains in RPMI medium before (co) and after exposure to 0.15 mM CHP stress at an OD₅₀₀ of 0.5. (G,H) The survival rates of the *S. aureus* COL WT, $\Delta katA$, $\Delta ahpC$, Δtpx and Δbcp mutants (G) and the *katA* (G), *ahpC*, *tpx* and *bcp* (H) complemented strains were determined at 2 and 4 h after exposure to 0.25 mM CHP relative to the untreated control, which was set to 100%. Mean values and SD of four to six biological replicates are presented. The statistics were calculated using Student’s unpaired two-tailed *t*-test in Graph Prism. Symbols: ns $p > 0.05$, * $p \leq 0.05$, ** $p \leq 0.01$ and *** $p \leq 0.001$.

3.8. Peroxiredoxin-Deficient $\Delta ahpC$, Δtpx and Δbcp Mutants Are Delayed in CHP Detoxification as Revealed by Brx-roGFP2 Measurements

To investigate the impact of the peroxiredoxins in the maintenance of the reduced state of E_{BSH} in *S. aureus*, Brx-roGFP2 biosensor measurements were performed after 0.5 mM CHP stress (Figure 7). The Brx-roGFP2 biosensor was similarly quickly oxidized by 0.5 mM CHP in the WT, $\Delta katA$, $\Delta ahpC$, Δtpx and Δbcp mutants. However, while the WT and $\Delta katA$ mutant could regenerate the reduced state of E_{BSH} within 2 h, the $\Delta ahpC$ mutant was unable to regenerate the basal level of E_{BSH} during the recovery phase from CHP stress (Figure 7A,B). In addition, both the Δbcp and Δtpx mutants showed significant delays in recovery of the reduced state of E_{BSH} upon CHP stress as compared to the WT (Figure 7C,D). These biosensor results support that the peroxiredoxins AhpC, Tpx and Bcp are important for CHP detoxification and contribute to regeneration of E_{BSH} during the recovery phase from CHP stress in *S. aureus*. In contrast, KatA does not contribute to CHP detoxification and resistance in *S. aureus*.

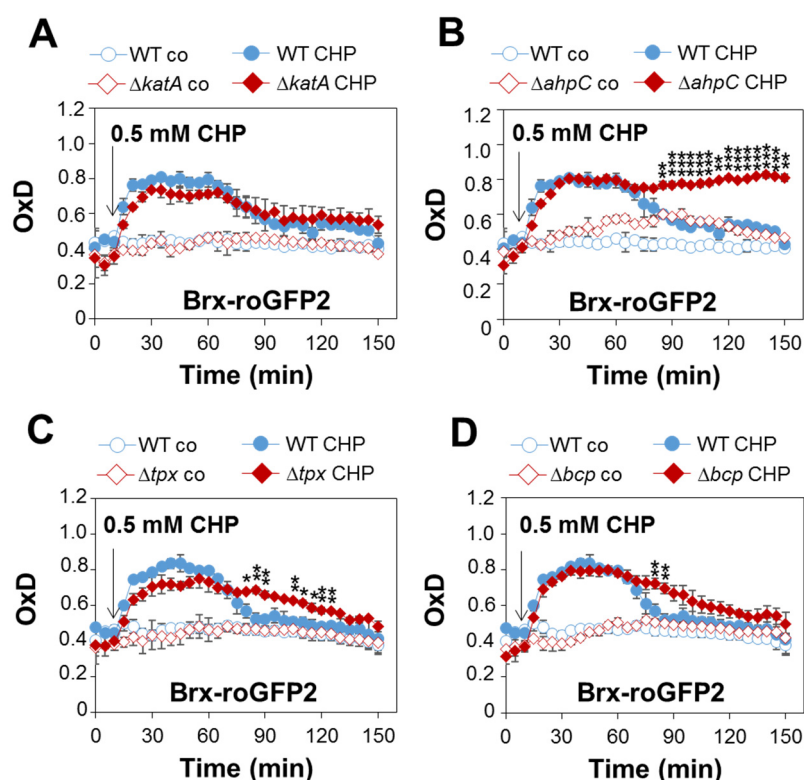


Figure 7. AhpC, Tpx and Bcp function in CHP detoxification and regeneration of reduced E_{BSH} during the recovery phase, as revealed by the Brx-roGFP2 biosensor. (A–D) Brx-roGFP2 responses to 0.5 mM CHP in *S. aureus* COL WT, $\Delta katA$ (A), $\Delta ahpC$ (B), Δtpx (C) and Δbcp mutants expressing Brx-roGFP2 from plasmid pRB473. H_2O_2 injection assays were performed in microplates and the biosensor responses measured using the CLARIOstar microplate reader, as described previously [45]. (D) The oxidation degree (OxD) of the Brx-roGFP2 response was calculated based on the 405/488 nm excitation ratio and normalized to fully reduced (DTT-treated) and oxidized (diamide-treated) controls. Mean values and SD of three biological replicates are shown. The statistics were calculated using Student's unpaired two-tailed *t*-test in Graph Prism. Symbols: ^{ns} $p > 0.05$, * $p \leq 0.05$, ** $p \leq 0.01$ and *** $p \leq 0.001$.

3.9. KatA and Peroxiredoxins Do Not Contribute to Protection against HOCl Stress

Previous transcriptome analyses revealed an increased transcription of the PerR regulon under HOCl stress in *S. aureus* [38]. Thus, growth curves and survival assays were used to analyse the phenotypes of the $\Delta katA$, $\Delta ahpC$, Δtpx and Δbcp mutants under HOCl stress. However, none of these mutants showed significant defects in growth or survival after HOCl stress compared to the WT, indicating that the catalase and peroxiredoxins do not contribute to HOCl detoxification and resistance in *S. aureus* (Figure S5A–E).

4. Discussion

Here, we investigated the roles of catalase and peroxiredoxins in the peroxide stress resistance and priming of *S. aureus* during aerobic and microaerophilic growth. Our results revealed that *S. aureus* is not primable towards improved H_2O_2 resistance during aerobic growth due to its constitutive H_2O_2 resistance, which was shown to be dependent on the catalase KatA. Moreover, we found that microaerophilic *S. aureus* cells can be primed to acquire an enhanced resistance towards lethal H_2O_2 doses, which was also mediated by KatA (Figure 3B,D). In addition, the peroxiredoxins AhpC, Tpx and Bcp were shown to contribute to the CHP detoxification and resistance in *S. aureus* to ensure the maintenance of the redox balance upon recovery from stress.

The roles of KatA and AhpC in the peroxide resistance of *S. aureus* have been previously demonstrated [20]. In this work, we additionally used Brx-roGFP2 biosensor measurements,

showing the impact of KatA and AhpC on the level of H₂O₂ detoxification and regeneration of reduced E_{BSH} under oxidative stress. Without KatA, *S. aureus* cells are highly sensitive to oxidants and only able to remove low doses of 0.4 mM H₂O₂, which were shown to be detoxified by AhpC. In addition, the $\Delta\text{ahpC}\Delta\text{katA}$ double mutant showed an increased sensitivity towards H₂O₂ stress in survival assays as compared to the ΔkatA mutant. These data confirm that KatA and AhpCF have compensatory roles in H₂O₂ resistance to ensure the survival of *S. aureus* under oxidative stress [20]. Expression of *katA*, *bcp*, *dps* and the *ahpCF* operon is controlled by the peroxide-sensing PerR repressor, which is inactivated by H₂O₂ due to Fe²⁺-catalysed histidine oxidation in *S. aureus* [18,52,53]. Due to PerR derepression in the ΔahpC mutant, *katA* and *dps* expression was elevated, as confirmed here using Northern blots and shown previously [20]. Thus, the higher KatA expression level in the ΔahpC mutant mediates the enhanced H₂O₂ resistance, confirming previous results in *S. aureus* and *B. subtilis* [20,54,55].

In addition, we showed that aerobically grown *S. aureus* acquire an improved resistance to H₂O₂ during the stationary phase, which also depends on KatA. The oxidative stress resistance was also enhanced during the stationary phase in other bacteria, such as *B. subtilis* and *E. coli* [56,57]. In addition, KatA activity was elevated during the stationary phase in *S. aureus* and *B. subtilis* [20,48]. Altogether, our results on aerobic *S. aureus* cells reveal that KatA is the major player that confers the strong constitutive H₂O₂ resistance during the log and stationary phases, while the peroxiredoxin AhpC plays an additional role of scavenging 0.4 mM H₂O₂ in the absence of KatA. Apart from its major role as an H₂O₂ scavenger, the catalase also provides heme and iron as cofactors for cellular metabolism, which could contribute to *S. aureus* survival under oxidative stress.

We further showed that *S. aureus* is primable with sub-lethal doses of 0.1 mM H₂O₂ to acquire an improved resistance towards otherwise lethal doses of 10 mM H₂O₂ during the microaerophilic growth. This microaerophilic H₂O₂ priming was found to be dependent on KatA, which was transcriptionally induced and showed a higher catalase activity upon challenge with the priming dose. These results are consistent with previous data showing increased KatA activity by exposure to 100 μM H₂O₂ during oxygen limitation [52]. We showed that microaerophilic priming by KatA prepares the cells to better survive the lethal triggering stress, resulting in improved growth and survival of *S. aureus*. In contrast, due to their constitutive H₂O₂ resistance, aerobic *S. aureus* cells were not primable to acquire higher resistance towards lethal H₂O₂ doses. Aerobic priming was not possible with 0.1 mM or 1 mM H₂O₂ since *katA* transcription and catalase activity were already elevated in naïve cells and could not be further increased in primed cells. The higher basal level of E_{BSH} of -291 mV in aerobic cells compared to the more reducing basal E_{BSH} of -310 mV in microaerophilic cells strongly indicates an increased ROS level in aerobic cells due to aerobic respiration. These biosensor data support that *S. aureus* is primed by endogenous ROS generated by aerobic respiration to achieve their constitutive H₂O₂ resistance phenotype (Figure 8). Thus, the PerR regulon is already up-regulated during aerobic growth due to ROS generated during aerobic respiration [52], resulting in the H₂O₂-resistant phenotype.

This up-regulation of the PerR regulon in *S. aureus* during the aerobic growth was caused by the hypersensitive PerR repressor, which is poised by very low endogenous levels of H₂O₂ generated during aerobic respiration [52]. The endogenous H₂O₂ concentration in aerobic *E. coli* cells was determined as ~ 50 nM [58]. While PerR of *S. aureus* is hypersensitive to endogenous H₂O₂ levels during aerobic growth, the PerR protein of *B. subtilis* is less sensitive and cannot sense such low H₂O₂ levels originating from aerobic respiration [52]. Thus, *B. subtilis* can be primed during aerobic growth with 0.1 mM H₂O₂, leading to PerR inactivation and derepression of the PerR-controlled KatA, which confers an adaptive resistance against the otherwise lethal triggering dose of 10 mM H₂O₂ [33,34,52,55,59].

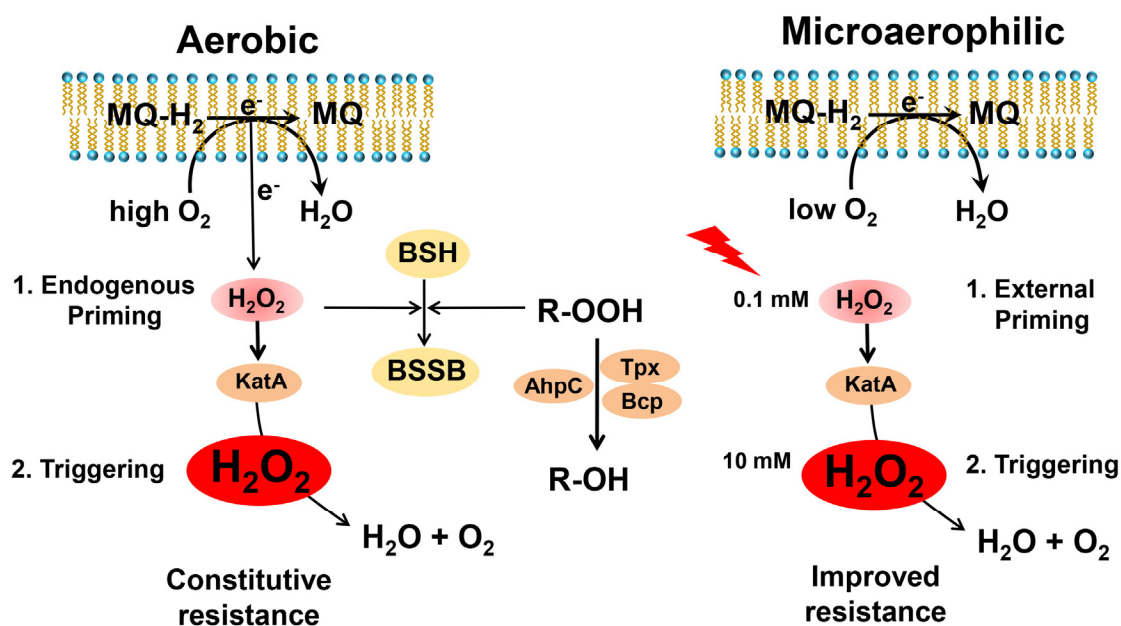


Figure 8. Summary schematics of microaerophilic H_2O_2 priming (right) and constitutive aerobic H_2O_2 resistance (left) in *S. aureus*. We found that microaerophilic priming with $100 \mu\text{M}$ H_2O_2 induces improved resistance towards otherwise lethal doses of 10 mM H_2O_2 in *S. aureus* (right), while aerobic cells are already primed by endogenous ROS originating from respiration, resulting in the constitutive high H_2O_2 resistance (left). The higher ROS levels during the aerobic growth were revealed by the $\sim 20 \text{ mV}$ increased basal E_{BSH} compared to microaerophilic cells. The catalase KatA was shown to be induced upon microaerophilic H_2O_2 priming (right) and by endogenous H_2O_2 during aerobic respiration (left), mediating improved and constitutive H_2O_2 resistance, respectively, in *S. aureus*. In addition, the peroxiredoxins AhpC, Tpx and Bcp were shown to confer resistance towards organic hydroperoxides (R-OOH). Furthermore, KatA and the peroxiredoxins contribute to the regeneration of reduced E_{BSH} upon recovery from oxidative stress. MQ-H₂ and MQ indicate reduced and oxidized menaquinone. BSH and BSSB are reduced bacillithiol and oxidized bacillithiol disulfide, respectively.

Similarly, aerobic priming is possible in *E. coli* and *S. Typhimurium* after exposure to $100 \mu\text{M}$ H_2O_2 , leading to activation of the OxyR regulon, including the major catalase, which confers an adaptive and improved resistance towards lethal concentrations of 10 mM H_2O_2 [36,57,60]. In conclusion, priming of bacteria towards improved H_2O_2 resistance depends on the sensitivity of the redox-sensing peroxide regulators. While many bacteria harbour less sensitive H_2O_2 sensors and are primable by sub-lethal H_2O_2 doses during aerobic growth, *S. aureus* PerR is hypersensitive to endogenous H_2O_2 levels during aerobic growth [52], resulting in constitutive aerobic H_2O_2 resistance and microaerophilic priming to acquire improved H_2O_2 resistance only in oxygen-limited conditions (Figure 8).

While KatA is responsible for detoxification of up to 100 mM H_2O_2 and confers the high resistance to 100 mM H_2O_2 in aerobic *S. aureus* cells, the peroxiredoxin AhpC was shown to enable the detoxification of low levels of 0.4 mM H_2O_2 , which could originate from the aerobic respiration. Thus, our results support that catalases are scavengers of high mM levels of H_2O_2 , whereas peroxiredoxins can only detoxify physiological μM H_2O_2 levels. However, the levels of H_2O_2 experienced by *S. aureus* during the oxidative burst were determined in the range of $\sim 2 \mu\text{M}$ inside the phagosomes of neutrophils and macrophages [13,61,62]. In mammalian cells, the physiological intracellular H_2O_2 concentration was estimated in the range of $1\text{--}100 \text{ nM}$, while the extracellular H_2O_2 was 100-fold higher [63]. Thus, *S. aureus* might not experience such high doses of $10\text{--}100 \text{ mM}$ H_2O_2 during interaction with immune cells. However, as a commensal bacterium, *S. aureus* colonizes the anterior nares and the nasopharynx together with competing microbes, such as *Streptococcus pneumoniae*, which generates millimolar levels of H_2O_2 by the lactate and

pyruvate oxidases to kill competitive bacteria [64–69]. In a mouse infection model, KatA was required for nasal colonization of *S. aureus* [18]. Furthermore, the *katA* mutant was impaired in survival towards H₂O₂ produced by *S. pneumoniae* during nasal colonization [20,70]. Thus, microaerophilic H₂O₂ priming of *S. aureus* might provide an advantage in its ecological niche to resist the high H₂O₂ levels generated by competing microbes.

In contrast, KatA and the peroxiredoxins are not directly involved in the defence against HOCl stress in *S. aureus*. However, KatA might contribute to lowering external H₂O₂ and, subsequently, HOCl levels in the neutrophil phagosome. In support of this notion, KatA was found to be induced upon macrophage infection and to be essential for survival of *S. aureus* inside macrophages [21]. In addition, *S. aureus* strains with high catalase activity were more resistant to killing by neutrophils compared to strains with lower catalase activity [22]. These data support that KatA is an important defence mechanism in *S. aureus* against the respiratory burst of macrophages and neutrophils.

In addition, the peroxiredoxins AhpC, Tpx and Bcp were found to confer protection against CHP stress in *S. aureus* cells. Using Brx-roGFP2 biosensor measurements, the peroxiredoxin-deficient Δ *ahpC*, Δ *tpx* and Δ *bcp* mutants showed delayed regeneration of the reduced state of E_{B_{SH}} after recovery from CHP stress. Thus, AhpC, Tpx and Bcp function in CHP detoxification and contribute to the maintenance of the cellular redox balance. The role of AhpC in CHP resistance has been previously demonstrated in *S. aureus* [20]. Similarly, the AhpC homologs of *B. subtilis*, *E. coli* and *S. Typhimurium* conferred resistance towards CHP stress [55,71]. In *E. coli*, the Δ *tpx* and Δ *bcp* mutants were more sensitive towards various OHPs, indicating that these peroxiredoxins are more specific to reduction of organic peroxide substrates [26,28]. Kinetic assays of the *E. coli* Tpx protein demonstrated the substrate specificity towards alkyl hydroperoxides over H₂O₂ [27]. Similarly, Bcp of *E. coli* has a fivefold higher V_{max}/K_m value for linoleic acid hydroperoxide as a substrate compared to H₂O₂ [26].

5. Conclusions

Taken together, we have shown that the catalase KatA is the major player in aerobic H₂O₂ resistance in *S. aureus* and mediates priming to endogenous ROS levels generated during aerobic respiration to confer the constitutive H₂O₂ resistance towards the triggering stimulus in aerobic cells. In addition, KatA mediates microaerophilic priming by low H₂O₂ levels to prepare *S. aureus* cells for improved and adaptive resistance against otherwise lethal H₂O₂ doses. Furthermore, the peroxiredoxins AhpC, Tpx and Bcp were shown to contribute to CHP detoxification and resistance to ensure the survival and regeneration of the reduced E_{B_{SH}} in *S. aureus* (Figure 8). In future studies, we aim to elucidate the functions of KatA and the peroxiredoxins in signal transduction, as redox-active chaperones and in cellular metabolism during aerobic growth and under oxidative stress in *S. aureus*.

Supplementary Materials: The following supporting information can be downloaded at: <https://www.mdpi.com/article/10.3390/antiox11091793/s1>: Figure S1: Complementation of KatA increases H₂O₂ resistance in *S. aureus*, but the catalase activity in the *katA* complemented strain is lower compared to the WT. Figure S2: Growth and catalase activity of the *ahpC* complemented strain. Figure S3: The Δ *katA* Δ *ahpC* double mutant is hypersensitive towards H₂O₂ and delayed in the recovery of reduced E_{B_{SH}} after 0.4 mM H₂O₂. Figure S4: The *katA* complemented strain is not primable towards increased H₂O₂ resistance during microaerophilic growth. Figure S5: KatA and the peroxiredoxins AhpC, Tpx and Bcp are not involved in HOCl detoxification in *S. aureus*. Figure S6: The Northern blot images using the *katA* specific RNA probe show the *katA* transcripts (images of Figure 1H; two bioreplicates, three technical replicates). Figure S7: The Northern blot images using the *ahpC* specific RNA probe show the *ahpCF* operon transcripts (images of Figure 1H; two bioreplicates, three technical replicates). Figure S8: The Northern blot images using the *dps* specific RNA probe show the *dps* operon transcripts (images of Figure 1H; two bioreplicates, three technical replicates). Figure S9: The Northern blot images of priming experiments using the *katA* specific RNA probe show the *katA* transcripts (images of Figure 5B,C; three bioreplicates). Figure S10: The Northern blot images of priming experiments using the *ahpC* specific RNA probe show the *ahpCF*

transcripts (images of Figure 5B,C; three bioreplicates). Figure S11: Native gels of catalase stains used for KatA activity assays (images of Figure 5F; two bioreplicates, two technical replicates). Figure S12: Native gels of catalase stains used for KatA activity assays (images of Figure S1D; three bioreplicates). Figure S13: Native gels of catalase stains used for KatA activity assays (images of Figure S2B; three bioreplicates). Table S1: Bacterial strains; Table S2: Plasmids; Table S3: Oligonucleotide primers. Table S4: CFU counts for the H₂O₂ survival assays. Table S5: CFU counts for microaerophilic H₂O₂ priming. Table S6: CFU counts for aerobic H₂O₂ priming. Table S7: CFU counts for the CHP survival assays. Table S8: CFU counts for HOCl survival assays.

Author Contributions: N.L. and V.V.L. performed the experiments and analysed the data. V.V.L. constructed the mutants and provided advice for biosensor measurements. N.L. wrote the initial draft of the manuscript. H.A. designed the concept of the project, supervised the experiments, provided funding and wrote the final manuscript. All authors have read and agreed to the published version of the manuscript.

Funding: This work was supported by an ERC Consolidator grant (GA 615585) MYCOTHILOME and grants from the Deutsche Forschungsgemeinschaft (AN746/4-1 and AN746/4-2) within the project SPP1710, by the SFB973 project C08 and by the SFB/TR84 project B06 to H.A.

Institutional Review Board Statement: Not applicable.

Informed Consent Statement: Not applicable.

Data Availability Statement: All reported data are available in the manuscript.

Acknowledgments: We are very grateful to Franziska Kiele for excellent technical assistance. We further would like to thank Quach Ngoc Tung and Lukas Olf for their support in mutant constructions and phenotype analyses. The publication fee of this article was funded by the Open Access Initiative of the Freie Universität Berlin.

Conflicts of Interest: The authors declare no conflict of interest. The funders had no role in the design of the study; in the collection, analyses, or interpretation of data; in the writing of the manuscript; or in the decision to publish the results.

References

1. Archer, G.L. *Staphylococcus aureus*: A well-armed pathogen. *Clin. Infect Dis.* **1998**, *26*, 1179–1181. [[CrossRef](#)] [[PubMed](#)]
2. Lowy, F.D. *Staphylococcus aureus* infections. *N. Engl. J. Med.* **1998**, *339*, 520–532. [[CrossRef](#)] [[PubMed](#)]
3. Boucher, H.W.; Corey, G.R. Epidemiology of methicillin-resistant *Staphylococcus aureus*. *Clin. Infect Dis.* **2008**, *46* (Suppl. S5), S344–S349. [[CrossRef](#)] [[PubMed](#)]
4. Sies, H.; Belousov, V.V.; Chandel, N.S.; Davies, M.J.; Jones, D.P.; Mann, G.E.; Murphy, M.P.; Yamamoto, M.; Winterbourn, C. Defining roles of specific reactive oxygen species (ROS) in cell biology and physiology. *Nat. Rev. Mol. Cell Biol.* **2022**, *23*, 499–515. [[CrossRef](#)] [[PubMed](#)]
5. Dupre-Crochet, S.; Erard, M.; Nubetae, O. ROS production in phagocytes: Why, when, and where? *J. Leukoc. Biol.* **2013**, *94*, 657–670. [[CrossRef](#)]
6. Winterbourn, C.C.; Kettle, A.J.; Hampton, M.B. Reactive oxygen species and neutrophil function. *Annu. Rev. Biochem.* **2016**, *85*, 765–792. [[CrossRef](#)] [[PubMed](#)]
7. Nguyen, G.T.; Green, E.R.; Meccas, J. Neutrophils to the ROScue: Mechanisms of NADPH Oxidase Activation and Bacterial Resistance. *Front. Cell Infect Microbiol.* **2017**, *7*, 373. [[CrossRef](#)] [[PubMed](#)]
8. Herb, M.; Schramm, M. Functions of ROS in Macrophages and Antimicrobial Immunity. *Antioxidants* **2021**, *10*, 313. [[CrossRef](#)]
9. Ulfing, A.; Leichert, L.I. The effects of neutrophil-generated hypochlorous acid and other hypohalous acids on host and pathogens. *Cell Mol. Life Sci.* **2021**, *78*, 385–414. [[CrossRef](#)]
10. Winterbourn, C.C.; Kettle, A.J. Redox reactions and microbial killing in the neutrophil phagosome. *Antioxid Redox Signal* **2013**, *18*, 642–660. [[CrossRef](#)]
11. Petersen, S.V.; Poulsen, N.B.; Linneberg Matthiesen, C.; Vilhardt, F. Novel and Converging Ways of NOX2 and SOD3 in Trafficking and Redox Signaling in Macrophages. *Antioxidants* **2021**, *10*, 172. [[CrossRef](#)]
12. Imlay, J.A. Pathways of oxidative damage. *Annu. Rev. Microbiol.* **2003**, *57*, 395–418. [[CrossRef](#)] [[PubMed](#)]
13. Imlay, J.A. Cellular defenses against superoxide and hydrogen peroxide. *Annu. Rev. Biochem.* **2008**, *77*, 755–776. [[CrossRef](#)] [[PubMed](#)]
14. Linzner, N.; Loi, V.V.; Fritsch, V.N.; Antelmann, H. Thiol-based redox switches in the major pathogen *Staphylococcus aureus*. *Biol. Chem.* **2021**, *402*, 333–361. [[CrossRef](#)] [[PubMed](#)]
15. Hillion, M.; Antelmann, H. Thiol-based redox switches in prokaryotes. *Biol. Chem.* **2015**, *396*, 415–444. [[CrossRef](#)]

16. Linzner, N.; Loi, V.V.; Fritsch, V.N.; Tung, Q.N.; Stenzel, S.; Wirtz, M.; Hell, R.; Hamilton, C.J.; Tedin, K.; Fulde, M.; et al. *Staphylococcus aureus* uses the bacilliredoxin (BrxAB)/bacillithiol disulfide reductase (YpdA) redox pathway to defend against oxidative stress under infections. *Front. Microbiol.* **2019**, *10*, 1355. [[CrossRef](#)]
17. Loi, V.V.; Harms, M.; Müller, M.; Huyen, N.T.T.; Hamilton, C.J.; Hochgräfe, F.; Pane-Farre, J.; Antelmann, H. Real-time imaging of the bacillithiol redox potential in the human pathogen *Staphylococcus aureus* using a genetically encoded bacilliredoxin-fused redox biosensor. *Antioxid Redox Signal* **2017**, *26*, 835–848. [[CrossRef](#)]
18. Horsburgh, M.J.; Clements, M.O.; Crossley, H.; Ingham, E.; Foster, S.J. PerR controls oxidative stress resistance and iron storage proteins and is required for virulence in *Staphylococcus aureus*. *Infect Immun.* **2001**, *69*, 3744–3754. [[CrossRef](#)]
19. Weber, H.; Engelmann, S.; Becher, D.; Hecker, M. Oxidative stress triggers thiol oxidation in the glyceraldehyde-3-phosphate dehydrogenase of *Staphylococcus aureus*. *Mol. Microbiol.* **2004**, *52*, 133–140. [[CrossRef](#)]
20. Cosgrove, K.; Coutts, G.; Jonsson, I.M.; Tarkowski, A.; Kokai-Kun, J.F.; Mond, J.J.; Foster, S.J. Catalase (KatA) and alkyl hydroperoxide reductase (AhpC) have compensatory roles in peroxide stress resistance and are required for survival, persistence, and nasal colonization in *Staphylococcus aureus*. *J. Bacteriol.* **2007**, *189*, 1025–1035. [[CrossRef](#)]
21. Das, D.; Saha, S.S.; Bishayi, B. Intracellular survival of *Staphylococcus aureus*: Correlating production of catalase and superoxide dismutase with levels of inflammatory cytokines. *Inflamm. Res.* **2008**, *57*, 340–349. [[CrossRef](#)] [[PubMed](#)]
22. Mandell, G.L. Catalase, superoxide dismutase, and virulence of *Staphylococcus aureus*. In vitro and in vivo studies with emphasis on staphylococcal–leukocyte interaction. *J. Clin. Invest.* **1975**, *55*, 561–566. [[CrossRef](#)] [[PubMed](#)]
23. Meireles, D.A.; da Silva Neto, J.F.; Domingos, R.M.; Alegria, T.G.P.; Santos, L.C.M.; Netto, L.E.S. Ohr–OhrR, a neglected and highly efficient antioxidant system: Structure, catalysis, phylogeny, regulation, and physiological roles. *Free Radic Biol. Med.* **2022**, *185*, 6–24. [[CrossRef](#)] [[PubMed](#)]
24. Poole, L.B.; Hall, A.; Nelson, K.J. Overview of peroxiredoxins in oxidant defense and redox regulation. *Curr. Protoc. Toxicol.* **2011**, *7*, 9. [[CrossRef](#)] [[PubMed](#)]
25. Parsonage, D.; Nelson, K.J.; Ferrer-Sueta, G.; Alley, S.; Karplus, P.A.; Furdui, C.M.; Poole, L.B. Dissecting peroxiredoxin catalysis: Separating binding, peroxidation, and resolution for a bacterial AhpC. *Biochemistry* **2015**, *54*, 1567–1575. [[CrossRef](#)] [[PubMed](#)]
26. Jeong, W.; Cha, M.K.; Kim, I.H. Thioredoxin-dependent hydroperoxide peroxidase activity of bacterioferritin comigratory protein (BCP) as a new member of the thiol-specific antioxidant protein (TSA)/Alkyl hydroperoxide peroxidase C (AhpC) family. *J. Biol. Chem.* **2000**, *275*, 2924–2930. [[CrossRef](#)]
27. Baker, L.M.; Poole, L.B. Catalytic mechanism of thiol peroxidase from *Escherichia coli*. Sulfenic acid formation and overoxidation of essential CYS61. *J. Biol. Chem.* **2003**, *278*, 9203–9211. [[CrossRef](#)]
28. Cha, M.K.; Kim, W.C.; Lim, C.J.; Kim, K.; Kim, I.H. *Escherichia coli* periplasmic thiol peroxidase acts as lipid hydroperoxide peroxidase and the principal antioxidative function during anaerobic growth. *J. Biol. Chem.* **2004**, *279*, 8769–8778. [[CrossRef](#)]
29. Imber, M.; Huyen, N.T.T.; Pietrzyk-Brzezinska, A.J.; Loi, V.V.; Hillion, M.; Bernhardt, J.; Thärichen, L.; Kolsek, K.; Saleh, M.; Hamilton, C.J.; et al. Protein S-bacillithiolation functions in thiol protection and redox regulation of the glyceraldehyde-3-phosphate dehydrogenase Gap in *Staphylococcus aureus* under hypochlorite stress. *Antioxid Redox Signal* **2018**, *28*, 410–430. [[CrossRef](#)]
30. Chelikani, P.; Fita, I.; Loewen, P.C. Diversity of structures and properties among catalases. *Cell Mol. Life Sci.* **2004**, *61*, 192–208. [[CrossRef](#)]
31. Mongkolsuk, S.; Helmann, J.D. Regulation of inducible peroxide stress responses. *Mol. Microbiol.* **2002**, *45*, 9–15. [[CrossRef](#)] [[PubMed](#)]
32. Faulkner, M.J.; Helmann, J.D. Peroxide stress elicits adaptive changes in bacterial metal ion homeostasis. *Antioxid Redox Signal* **2011**, *15*, 175–189. [[CrossRef](#)] [[PubMed](#)]
33. Engelmann, S.; Hecker, M. Impaired oxidative stress resistance of *Bacillus subtilis sigB* mutants and the role of *katA* and *katE*. *FEMS Microbiol. Lett.* **1996**, *145*, 63–69. [[CrossRef](#)] [[PubMed](#)]
34. Murphy, P.; Dowds, B.C.; McConnell, D.J.; Devine, K.M. Oxidative stress and growth temperature in *Bacillus subtilis*. *J. Bacteriol.* **1987**, *169*, 5766–5770. [[CrossRef](#)]
35. Hilker, M.; Schwachtje, J.; Baier, M.; Balazadeh, S.; Baurle, I.; Geiselhardt, S.; Hinch, D.K.; Kunze, R.; Mueller-Roeber, B.; Rillig, M.C.; et al. Priming and memory of stress responses in organisms lacking a nervous system. *Biol. Rev. Camb. Philos. Soc.* **2016**, *91*, 1118–1133. [[CrossRef](#)]
36. Christman, M.F.; Morgan, R.W.; Jacobson, F.S.; Ames, B.N. Positive control of a regulon for defenses against oxidative stress and some heat-shock proteins in *Salmonella typhimurium*. *Cell* **1985**, *41*, 753–762. [[CrossRef](#)]
37. Chiang, S.M.; Schellhorn, H.E. Regulators of oxidative stress response genes in *Escherichia coli* and their functional conservation in bacteria. *Arch. Biochem. Biophys.* **2012**, *525*, 161–169. [[CrossRef](#)]
38. Loi, V.V.; Busche, T.; Tedin, K.; Bernhardt, J.; Wollenhaupt, J.; Huyen, N.T.T.; Weise, C.; Kalinowski, J.; Wahl, M.C.; Fulde, M.; et al. Redox-sensing under hypochlorite stress and infection conditions by the Rrf2-family repressor HypR in *Staphylococcus aureus*. *Antioxid Redox Signal* **2018**, *29*, 615–636. [[CrossRef](#)]
39. Winter, J.; Ilbert, M.; Graf, P.C.; Ozcelik, D.; Jakob, U. Bleach activates a redox-regulated chaperone by oxidative protein unfolding. *Cell* **2008**, *135*, 691–701. [[CrossRef](#)]

40. Linzner, N.; Fritsch, V.N.; Busche, T.; Tung, Q.N.; Loi, V.V.; Bernhardt, J.; Kalinowski, J.; Antelmann, H. The plant-derived naphthoquinone lapachol causes an oxidative stress response in *Staphylococcus aureus*. *Free Radic. Biol. Med.* **2020**, *158*, 126–136. [[CrossRef](#)]
41. Arnaud, M.; Chastanet, A.; Debarbouille, M. New vector for efficient allelic replacement in naturally nontransformable, low-GC-content, gram-positive bacteria. *Appl. Environ. Microbiol.* **2004**, *70*, 6887–6891. [[CrossRef](#)] [[PubMed](#)]
42. Rosenblum, E.D.; Tyrone, S. Serology, density, and morphology of staphylococcal phages. *J. Bacteriol.* **1964**, *88*, 1737–1742. [[CrossRef](#)]
43. Fritsch, V.N.; Loi, V.V.; Busche, T.; Sommer, A.; Tedin, K.; Nürnberg, D.J.; Kalinowski, J.; Bernhardt, J.; Fulde, M.; Antelmann, H. The MarR-type repressor MhqR confers quinone and antimicrobial resistance in *Staphylococcus aureus*. *Antioxid Redox Signal* **2019**, *31*, 1235–1252. [[CrossRef](#)] [[PubMed](#)]
44. Fritsch, V.N.; Loi, V.V.; Busche, T.; Tung, Q.N.; Lill, R.; Horvatek, P.; Wolz, C.; Kalinowski, J.; Antelmann, H. The alarmone (p)ppGpp confers tolerance to oxidative stress during the stationary phase by maintenance of redox and iron homeostasis in *Staphylococcus aureus*. *Free Radic. Biol. Med.* **2020**, *161*, 351–364. [[CrossRef](#)] [[PubMed](#)]
45. Loi, V.V.; Antelmann, H. Method for measurement of bacillithiol redox potential changes using the Brx-roGFP2 redox biosensor in *Staphylococcus aureus*. *MethodsX* **2020**, *7*, 100900. [[CrossRef](#)]
46. Wetzstein, M.; Volker, U.; Dedio, J.; Lobau, S.; Zuber, U.; Schiesswohl, M.; Herget, C.; Hecker, M.; Schumann, W. Cloning, sequencing, and molecular analysis of the *dnaK* locus from *Bacillus subtilis*. *J. Bacteriol.* **1992**, *174*, 3300–3310. [[CrossRef](#)]
47. Clare, D.A.; Duong, M.N.; Darr, D.; Archibald, F.; Fridovich, I. Effects of molecular oxygen on detection of superoxide radical with nitroblue tetrazolium and on activity stains for catalase. *Anal. Biochem.* **1984**, *140*, 532–537. [[CrossRef](#)]
48. Loewen, P.C.; Switala, J. Multiple catalases in *Bacillus subtilis*. *J. Bacteriol.* **1987**, *169*, 3601–3607. [[CrossRef](#)]
49. Loi, V.V.; Busche, T.; Preuss, T.; Kalinowski, J.; Bernhardt, J.; Antelmann, H. The AGXX antimicrobial coating causes a thiol-specific oxidative stress response and protein S-bacillithiolation in *Staphylococcus aureus*. *Front. Microbiol.* **2018**, *9*, 3037. [[CrossRef](#)]
50. Loi, V.V.; Huyen, N.T.T.; Busche, T.; Tung, Q.N.; Gruhlke, M.C.H.; Kalinowski, J.; Bernhardt, J.; Slusarenko, A.J.; Antelmann, H. *Staphylococcus aureus* responds to allicin by global S-thioallylation—role of the Brx/BSH/YpdA pathway and the disulfide reductase MerA to overcome allicin stress. *Free Radic. Biol. Med.* **2019**, *139*, 55–69. [[CrossRef](#)]
51. Wolf, C.; Hochgräfe, F.; Kusch, H.; Albrecht, D.; Hecker, M.; Engelmann, S. Proteomic analysis of antioxidant strategies of *Staphylococcus aureus*: Diverse responses to different oxidants. *Proteomics* **2008**, *8*, 3139–3153. [[CrossRef](#)] [[PubMed](#)]
52. Ji, C.J.; Kim, J.H.; Won, Y.B.; Lee, Y.E.; Choi, T.W.; Ju, S.Y.; Youn, H.; Helmann, J.D.; Lee, J.W. *Staphylococcus aureus* PerR Is a hypersensitive hydrogen peroxide sensor using iron-mediated histidine oxidation. *J. Biol. Chem.* **2015**, *290*, 20374–20386. [[CrossRef](#)] [[PubMed](#)]
53. Lee, J.W.; Helmann, J.D. The PerR transcription factor senses H₂O₂ by metal-catalysed histidine oxidation. *Nature* **2006**, *440*, 363–367. [[CrossRef](#)] [[PubMed](#)]
54. Bsat, N.; Chen, L.; Helmann, J.D. Mutation of the *Bacillus subtilis* alkyl hydroperoxide reductase (*ahpCF*) operon reveals compensatory interactions among hydrogen peroxide stress genes. *J. Bacteriol.* **1996**, *178*, 6579–6586. [[CrossRef](#)]
55. Antelmann, H.; Engelmann, S.; Schmid, R.; Hecker, M. General and oxidative stress responses in *Bacillus subtilis*: Cloning, expression, and mutation of the alkyl hydroperoxide reductase operon. *J. Bacteriol.* **1996**, *178*, 6571–6578. [[CrossRef](#)] [[PubMed](#)]
56. Dowds, B.C.; Murphy, P.; McConnell, D.J.; Devine, K.M. Relationship among oxidative stress, growth cycle, and sporulation in *Bacillus subtilis*. *J. Bacteriol.* **1987**, *169*, 5771–5775. [[CrossRef](#)] [[PubMed](#)]
57. Farr, S.B.; Kogoma, T. Oxidative stress responses in *Escherichia coli* and *Salmonella typhimurium*. *Microbiol. Rev.* **1991**, *55*, 561–585. [[CrossRef](#)]
58. Seaver, L.C.; Imlay, J.A. Hydrogen peroxide fluxes and compartmentalization inside growing *Escherichia coli*. *J. Bacteriol.* **2001**, *183*, 7182–7189. [[CrossRef](#)]
59. Pinochet-Barros, A.; Helmann, J.D. Redox Sensing by Fe²⁺ in Bacterial Fur Family Metalloregulators. *Antioxid. Redox Signal* **2018**, *29*, 1858–1871. [[CrossRef](#)]
60. Åslund, F.; Zheng, M.; Beckwith, J.; Storz, G. Regulation of the OxyR transcription factor by hydrogen peroxide and the cellular thiol-disulfide status. *Proc. Natl. Acad. Sci. USA* **1999**, *96*, 6161–6165. [[CrossRef](#)]
61. Winterbourn, C.C.; Hampton, M.B.; Livesey, J.H.; Kettle, A.J. Modeling the reactions of superoxide and myeloperoxidase in the neutrophil phagosome: Implications for microbial killing. *J. Biol. Chem.* **2006**, *281*, 39860–39869. [[CrossRef](#)] [[PubMed](#)]
62. Imlay, J.A. Where in the world do bacteria experience oxidative stress? *Environ. Microbiol.* **2019**, *21*, 521–530. [[CrossRef](#)] [[PubMed](#)]
63. Sies, H.; Jones, D.P. Reactive oxygen species (ROS) as pleiotropic physiological signalling agents. *Nat. Rev. Mol. Cell Biol.* **2020**, *21*, 363–383. [[CrossRef](#)] [[PubMed](#)]
64. Bogaert, D.; de Groot, R.; Hermans, P.W.M. *Streptococcus pneumoniae* colonisation: The key to pneumococcal disease. *Lancet Infect. Dis.* **2004**, *4*, 144–154. [[CrossRef](#)]
65. Liu, C.M.; Price, L.B.; Hungate, B.A.; Abraham, A.G.; Larsen, L.A.; Christensen, K.; Stegger, M.; Skov, R.; Andersen, P.S. *Staphylococcus aureus* and the ecology of the nasal microbiome. *Sci. Adv.* **2015**, *1*, e1400216. [[CrossRef](#)]
66. Udaka, S.; Koukol, J.; Vennesland, B. Lactic oxidase of *Pneumococcus*. *J. Bacteriol.* **1959**, *78*, 714–725. [[CrossRef](#)]
67. Spellerberg, B.; Cundell, D.R.; Sandros, J.; Pearce, B.J.; Idanpaan-Heikkilä, I.; Rosenow, C.; Masure, H.R. Pyruvate oxidase, as a determinant of virulence in *Streptococcus pneumoniae*. *Mol. Microbiol.* **1996**, *19*, 803–813. [[CrossRef](#)]

68. Pericone, C.D.; Bae, D.; Shchepetov, M.; McCool, T.; Weiser, J.N. Short-sequence tandem and nontandem DNA repeats and endogenous hydrogen peroxide production contribute to genetic instability of *Streptococcus pneumoniae*. *J. Bacteriol.* **2002**, *184*, 4392–4399. [[CrossRef](#)]
69. Lisher, J.P.; Tsui, H.T.; Ramos-Montanez, S.; Hentchel, K.L.; Martin, J.E.; Trinidad, J.C.; Winkler, M.E.; Giedroc, D.P. Biological and chemical adaptation to endogenous hydrogen peroxide production in *Streptococcus pneumoniae* D39. *mSphere* **2017**, *2*, e00291-16. [[CrossRef](#)]
70. Park, B.; Nizet, V.; Liu, G.Y. Role of *Staphylococcus aureus* catalase in niche competition against *Streptococcus pneumoniae*. *J. Bacteriol.* **2008**, *190*, 2275–2278. [[CrossRef](#)]
71. Storz, G.; Jacobson, F.S.; Tartaglia, L.A.; Morgan, R.W.; Silveira, L.A.; Ames, B.N. An alkyl hydroperoxide reductase induced by oxidative stress in *Salmonella typhimurium* and *Escherichia coli*: Genetic characterization and cloning of ahp. *J. Bacteriol.* **1989**, *171*, 2049–2055. [[CrossRef](#)] [[PubMed](#)]